Neuron, Volume *106*

Supplemental Information

A Neuro-computational Account of Arbitration between Choice Imitation and Goal Emulation during Human Observational Learning

Caroline J. Charpentier, Kiyohito Iigaya, and John P. O'Doherty

Supplemental Information

Neuro-computational account of arbitration between choice imitation and goal emulation during human observational learning

		Imitation signals		Emulation signals				Arbitration signals	
		GLM2: Imitation reliability	GLM1: Imitation action value diff.	GLM2: Emulation reliability	GLM1: Token entropy	GLM1: Token KLdiv.	GLM1: Token RPE	GLM1: Reliability difference	GLM1: Chosen action value
Left TPJ pSTS	Study 1	-0.046 ±0.46	0.088* ±0.17	**0.172* ±0.55**	0.083* ±0.16	-0.010 ±0.17	0.042 ±0.14	**0.201* ±0.53**	0.032 ±0.23
	Study 2	-	-0.022 ±0.17	**0.195* ±0.55**	-0.112* ±0.25	-	-	**0.182* ±0.38**	-
Right TPJ pSTS	Study 1	0.041 ±0.65	0.088* ±0.21	0.299* ±0.66	0.121* ±0.26	0.046 ±0.21	-0.032 ±0.23	0.277* ±0.59	0.022 ±0.24
	Study 2	-	-0.038 ±0.22	0.137 ±0.78	-0.078 ±0.30	-	-	0.071 ±0.70	-
mOFC	Study 1	0.387* ±0.58	0.020 ±0.15	0.128 ±0.86	**-0.080* ±0.25**	-0.029 ±0.27	0.001 ±0.25	-0.059 ±0.85	**0.110* ±0.28**
	Study 2	0.077 ±0.28	-	-	**-0.107* ±0.19**	-	-	-	**0.109* ±0.22**
dmPFC	Study 1	-0.228 ±0.86	0.168* ±0.31	0.161 ±1.01	0.234* ±0.31	**0.201* ±0.23**	0.087 ±0.34	**0.383* ±0.89**	-0.095 ±0.41
	Study 2	-	-0.018 ±0.20	-	-0.061 ±0.27	**0.098* ±0.21**	-	**0.228* ±0.54**	-
PreSMA dACC	Study 1	-0.086 ±0.54	0.095* ±0.16	0.034 ±0.66	0.147* ±0.17	**0.170* ±0.18**	0.023 ±0.23	0.136 ±0.58	**-0.144* ±0.29**
	Study 2	-	0.025 ±0.12	-	-0.018 ±0.12	**0.123* ±0.17**	-	-	**-0.135* ±0.22**
Left vlPFC	Study 1	-0.007 ±0.78	0.130* ±0.27	0.187 ±0.76	0.133* ±0.26	0.066 ±0.24	0.116 ±0.29	0.209 ±0.68	-0.084 ±0.40
	Study 2	-	0.024 ±0.22	-	-0.077* ±0.22	-	-	-	-
Right vlPFC	Study 1	0.003 ±0.48	0.064* ±0.19	**0.320* ±0.50**	0.118* ±0.14	0.048 ±0.18	0.006 ±0.16	0.250* ±0.48	0.002 ±0.26
	Study 2	-	-0.041 ±0.14	**0.186* ±0.39**	-0.045 ±0.18	-	-	0.035 ±0.43	-
Dorsal striatum	Study 1	-0.052 ±0.30	0.052* ±0.10	-0.029 ±0.38	0.052* ±0.12	**0.043* ±0.09**	0.071* ±0.08	0.043 ±0.30	-0.004 ±0.16
	Study 2	-	-0.013 ±0.068	-	-0.022 ±0.08	**0.033* ±0.09**	-0.030 ±0.13	-	-

Table S1, related to Figures 4 & 5. Pre-registered ROI results. Betas associated with the preregistered contrasts from SPM GLM 1 and 2 were extracted from the preregistered ROIs (average across all voxels in ROI) for each subject. This table reports the mean betas ± standard deviation across subjects, separately for each study. In Study 1, every contrast was examined in every ROI as a way to generate hypotheses. In Study 2, only significant effects from Study 1 were examined. * $P<0.05$, t-tests and permutation tests. Results highlighted in bold indicate replication (significant effects in the same direction) across studies.

Region	Study 1					Study 2			
	x	y	z	Cluster size	T_{S1}	$Beta_{S2}$ (mean)	SD_{S2}	T_{S2}	P_{S2}
Imitation reliability (>0)									
mOFC, vmPFC, ACC	3	37	-7	325	5.01	0.038	0.35	0.59	0.28
Imitation reliability (<0)									
Right inferior Parietal / Angular gyrus	48	-46	58	107	4.43	-0.065	0.59	-0.61	0.27
Imitation action value difference (>0)									
Right dlPFC	30	24	41	333	5.82	-0.017	0.14	-0.69	0.25
Right TPJ	48	-49	36	333	5.39	-0.016	0.30	-0.29	0.39
Pre-SMA / dmPFC	-5	24	53	193	4.74	0.034	0.11	1.68	0.052
Left dlPFC	-43	19	41	101	4.64	0.072	0.24	1.64	0.056
Precuneus	3	-61	18	216	4.46	-0.050	0.18	-1.54	0.068
Left Thalamus	-15	-29	11	104	4.42	-0.012	0.08	-0.83	0.21
Left TPJ	-48	-59	36	275	4.28	0.008	0.32	0.13	0.45
Emulation reliability (>0)									
Right anterior Insula	**43**	**17**	**-12**	**126**	**4.82**	**0.258**	**0.43**	**3.28**	**<0.001**
Token entropy (>0)									
Bilateral inferior Parietal / Angular gyrus / TPJ / Precuneus	38	-49	46	3755	7.40	0.023	0.28	0.45	0.33
Right dlPFC / IFG / OFC / vlPFC	28	9	61	2875	6.20	-0.004	0.15	-0.16	0.44
Left dlPFC / IFG / OFC / vlPFC	-20	-4	63	2485	6.08	-0.024	0.16	-0.84	0.20
Cerebellum	-10	-79	-25	203	5.88	-0.002	0.12	-0.08	0.47
Right mid-Temporal	55	-41	-5	215	5.82	0.006	0.13	0.27	0.39
dmPFC / Pre-SMA/ dACC	-8	29	41	708	5.31	-0.029	0.17	-0.94	0.18
Thalamus	0	-16	3	191	4.95	-0.003	0.09	-0.14	0.44
Token KL divergence (>0)									
Left anterior Insula	**-33**	**14**	**-10**	**119**	**4.88**	**0.102**	**0.15**	**3.80**	**<0.001**
Right IFG / Precentral gyrus	**35**	**9**	**33**	**342**	**4.69**	**0.147**	**0.23**	**3.49**	**<0.001**
Right anterior Insula	**40**	**19**	**-2**	**122**	**4.65**	**0.117**	**0.15**	**4.41**	**<0.001**
Pre-SMA / dACC	**-8**	**19**	**46**	**140**	**4.44**	**0.174**	**0.22**	**4.30**	**<0.001**
Left IFG / Precentral gyrus	**-48**	**7**	**26**	**103**	**4.41**	**0.187**	**0.27**	**3.74**	**<0.001**
Right Supramarginal / inferior Parietal	**53**	**-39**	**46**	**109**	**4.09**	**0.246**	**0.38**	**3.56**	**<0.001**
Reliability difference – EM vs IM									
Right anterior Insula	**40**	**17**	**-12**	**113**	**5.97**	**0.099**	**0.28**	**1.95**	**0.031**
Right IFG	**45**	**4**	**21**	**184**	**5.02**	**0.173**	**0.51**	**1.87**	**0.036**
ACC / dmPFC	**13**	**44**	**26**	**91**	**4.80**	**0.089**	**0.23**	**2.09**	**0.023**
Right Angular gyrus	40	-74	48	206	4.38	0.225	0.74	1.67	0.052

Table S2, related to Figures 4 & 5. Replication findings using clusters from Study 1 group-level maps as functional ROIs in Study 2. Significant activation clusters from Study 1 (pre-registered) were identified following whole-brain cluster-level FWE correction at $p<0.05$ and cluster-forming threshold at $P<0.001$ uncorrected. Peak MNI coordinates are reported for Study 1, together with cluster size (number of contiguous voxels in the cluster) and peak voxel T-value. Each significant cluster was saved as a functional ROI, and mean signal from Study 2 was extracted in this ROI and averaged across subjects to assess replication. Mean beta, standard deviation and p-value (t-tests, also confirmed with permutation tests) are reported for Study 2. Regions highlighted in bold indicate replication at $P\leq0.05$.

	Study 1		Study 2	
	SPM GLM2	SPM GLM3	SPM GLM2	SPM GLM3
Left TPJ pSTS	0.366	**0.634**	0.028	**0.972**
Right TPJ pSTS	0.257	**0.743**	0.159	**0.841**
mOFC	0.047	**0.953**	0.013	**0.987**
dmPFC	**0.519**	0.481	0.031	**0.969**
PreSMA dACC	0.110	**0.890**	0.009	**0.991**
Left vlPFC	0.201	**0.799**	0.085	**0.915**
Right vlPFC	0.029	**0.971**	0.050	**0.950**
Dorsal striatum	0.035	**0.965**	0.019	**0.981**

Table S3, related to Figures 6 & 7. Exceedance probabilities from Bayesian fMRI model selection in pre-registered ROIs. After performing the Bayesian model selection analysis between SPM GLM2 and SPM GLM3, we averaged the exceedance probability associated with each model across all voxels of a given ROI. For each ROI, this exceedance probability represents the posterior probability that a model is more frequent than the other. For all ROIs and across both studies (except in the dmPFC in Study 1), SPM GLM3 was found to explain variations in the BOLD signal substantially better than SPM GLM2. In the dmPFC in Study 1, the performance of both models was equivalent.

Contrast & Region	**x**	**y**	**z**	**Cluster size**	**T_{S1}**	**T_{S2}**
Arbitration signal (emulation reliability)						
ACC	0	39	3	155	4.34	4.14
Right vlPFC / insula	53	32	1	376	3.76	3.71
Right mid/sup temporal	48	-21	-7	61	3.84	3.67
Left postcentral / supramarginal	-58	-29	18	207	3.49	3.99
Right supramarginal / inferior parietal	65	-31	26	185	3.65	3.67
Left fusiform gyrus	-25	-71	-15	146	3.77	3.50
Right fusiform gyrus	30	-69	-10	69	3.67	3.42
dACC	5	17	31	31	3.71	3.42
Mid-cingulate cortex	15	-21	41	58	3.29	3.42
Left insula	-40	-9	-7	177	3.72	3.41
Left anterior insula	-43	12	-12	34	3.11	3.39
SMA / preSMA	8	-9	76	143	3.36	3.67
Left pSTS/TPJ	-58	-54	13	68	3.05	3.14
Emulation learning signal (token KL divergence) during feedback						
Left anterior insula	-35	17	-7	117	4.50	4.17
Right anterior insula	35	19	-10	179	3.81	4.25
Right IFG	43	9	26	328	3.64	3.33
Left IFG	-40	7	28	171	3.37	3.33
Right caudate / thalamus	8	-1	8	106	3.95	3.69
Left fusiform gyrus	-35	-56	-15	37	4.13	3.87
Right inferior occipital	30	-86	-10	54	3.31	3.80
Left inf-sup parietal / precuneus	-25	-71	38	389	3.60	4.47
Right superior occipital / parietal	28	-61	41	38	3.28	3.73
Right inferior parietal	50	-34	46	187	3.32	3.27
Right occipital / cuneus	18	-76	6	345	3.41	3.47
Left mid-sup frontal / precentral	-23	2	51	169	3.30	3.38
Right mid-sup frontal / precentral	30	9	58	136	3.34	3.18
SMA / preSMA	5	22	48	351	3.80	3.77
Right TPJ / pSTS	55	-44	23	44	3.28	3.22

Imitation learning signal (action change) during feedback						
SMA / preSMA	-5	4	66	47	3.21	3.11
Left inferior parietal	-38	-54	41	318	3.66	3.65
Right inferior parietal	50	-39	48	129	3.63	3.55
Left dlPFC	-45	32	31	53	3.46	3.59
Left anterior insula	-35	22	-10	45	3.47	3.43
Left mid-sup frontal / precentral	-18	14	63	119	3.23	3.18
Left IFG	-45	4	26	35	2.95	3.38
Precuneus	20	-69	61	34	2.75	2.74
Previous action unavailable > available during slot machine presentation						
SMA / preSMA	-8	12	51	1132	5.18	5.17
Left anterior insula	-35	22	-2	237	5.35	5.08
Right anterior insula	38	24	-2	253	4.89	4.63
Left IFG	-45	4	28	531	4.97	5.04
Right IFG	45	7	26	270	4.38	4.46
Left sup occipital / inf-sup parietal	-33	-84	28	1077	4.22	4.21
Right inf-sup parietal / occipital	53	-36	48	1505	4.45	4.52
Right mid-sup frontal / precentral	28	-6	53	408	4.12	4.18
Right inferior temporal	50	-56	-10	153	4.20	3.98
Left occipital / cuneus	-15	-81	3	58	3.82	3.06
Right occipital / cuneus	15	-69	13	50	4.31	3.31
Left caudate	-10	2	3	47	3.45	3.44
Right caudate	15	12	1	54	3.97	3.36
Left inferior parietal	-50	-41	43	54	3.25	4.08
Right cuneus / precuneus	23	-59	21	46	3.31	3.48
Right dlPFC	48	32	26	60	3.29	3.63
Left inferior occipital/temporal / fusiform	-38	-71	-12	168	3.33	3.71
Right fusiform gyrus	30	-71	-12	32	3.37	3.17
Token value during token presentation						
ACC	-8	39	-2	58	4.26	3.78
mOFC / vmPFC	-10	64	1	30	3.02	2.89
Emulation choice probability during self-choice (p<0.001 unc)						
mOFC / vmPFC	*-8*	*59*	*-10*	*210*	2.75	2.96
Negative Imitation choice probability during self-choice (p<0.001 unc)						
Right anterior insula	*38*	*29*	*-2*	*67*	2.87	3.46
dmPFC / preSMA / SMA	*3*	*24*	*43*	*64*	2.59	2.63

Table S4, related to Figures 6 & 7. SPM GLM3 conjunction analyses results. Conjunction maps between the second-level T-maps of studies 1 and 2 were thresholded at $P_{conjunction}<0.0001$ uncorrected, followed by whole-brain cluster level family-wise error correction at $P_{FWE}<0.05$ (equivalent to cluster size $k\geq30$ contiguous voxels). For the last two contrasts, emulation choice probability and negative imitation choice probability, no cluster survived the above threshold so a slightly more lenient cluster-forming threshold of $P_{conjunction}<0.001$ uncorrected was used for exploratory purposes. x, y, z represent MNI coordinates. T_{S1} and T_{S2} denote the T-value for Study 1 and Study 2, respectively. mOFC: medial orbitofrontal cortex. vmPFC: ventromedial prefrontal cortex. ACC: anterior cingulate cortex. IFG: inferior frontal gyrus. SMA: supplementary motor area. dmPFC: dorsomedial prefrontal cortex. dlPFC: dorsolateral prefrontal cortex. TPJ: temporoparietal junction. pSTS: posterior superior temporal sulcus.

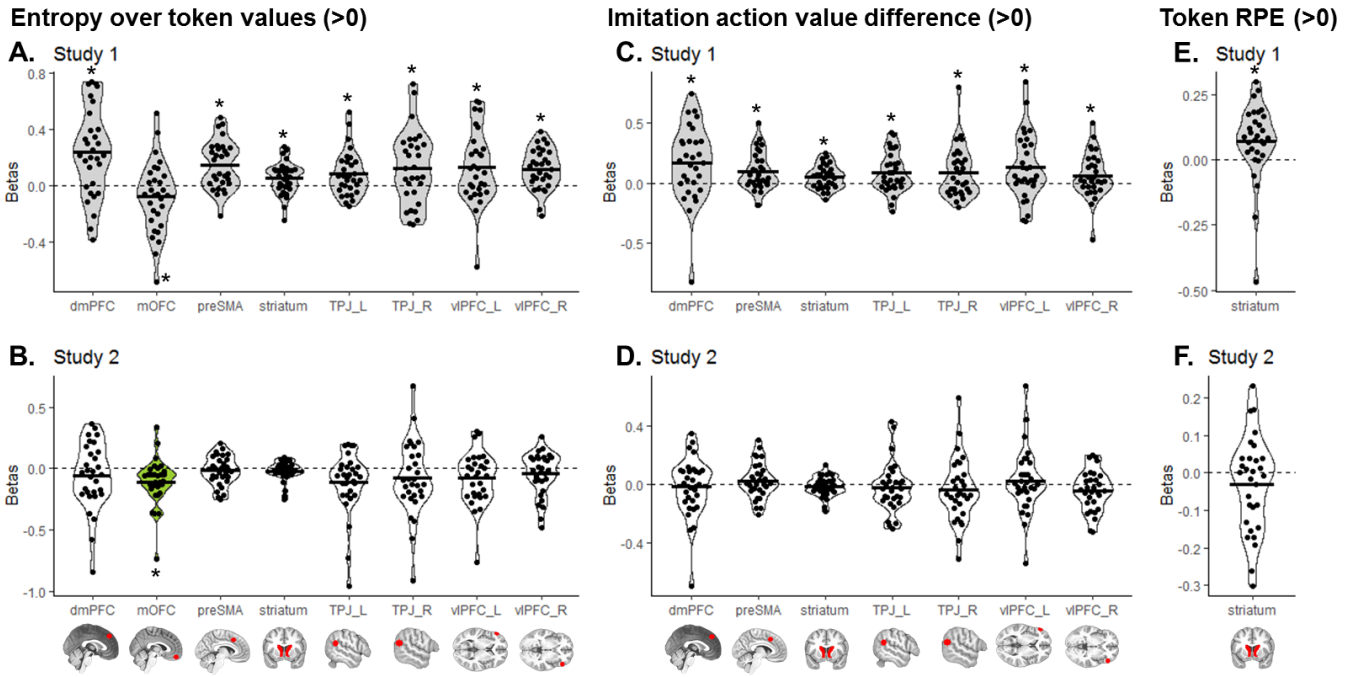

Figure S1, related to Figures 4 & 5. Pre-registered ROI results – additional contrasts. For the remaining contrasts in SPM GLM1 and GLM2 not shown on main text **Figures 4-5**, mean signal was extracted from each pre-registered ROI. Regions with significant signals in Study 1, plotted in grey, were selected as hypotheses and a priori ROI for Study 2. Green plots represent significant effects in Study 2, confirming the a priori hypothesis from Study 1. White plots represent hypotheses that were not confirmed in Study 2. Dots represent individual subjects and the black bar represents the mean beta value for each regressor. T-tests: * P<0.05. The same results were found using non-parametric permutation tests.

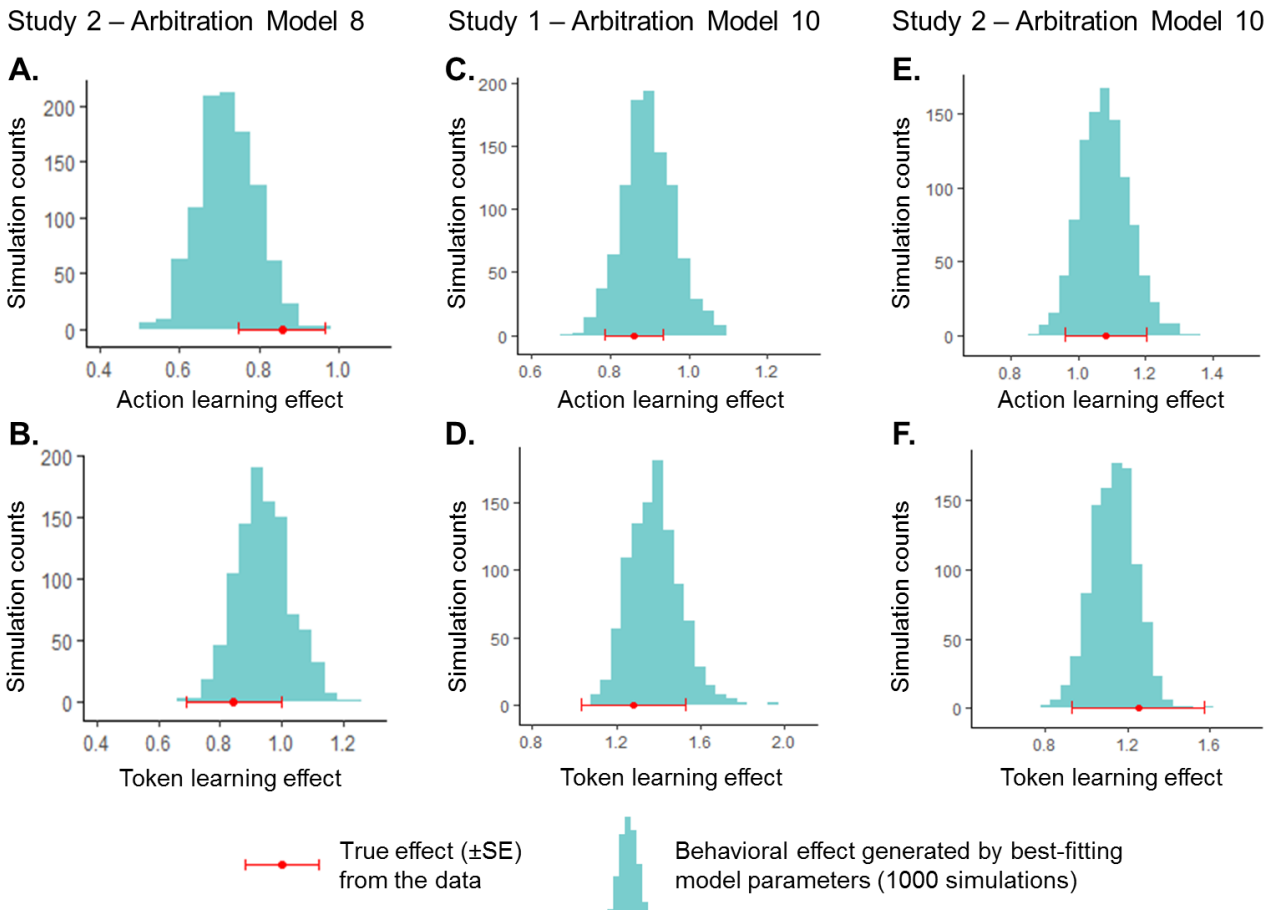

Figure S2, related to Table 1 & Figure 2. Action and token learning effects are captured by the different arbitration models. (**A-B**) Arbitration Model 8, which outperformed Model 7 in Study 2 based on BIC values, was able to capture the two behavioral effects obtained by a simple logistic regression: the action learning effect (**A**) and the token learning effect (**B**). (**C-F**) Arbitration Model 10, which arbitrates between the original emulation strategy and a simpler 1-step imitation strategy and outperformed Arbitration Models 7 and 8 in both studies, was also able to capture the action learning effect (**C, E**) and the token learning effect (**D, F**), in both Study 1 (**C, D**) and Study 2 (**E, F**). The red data point above the X-axis depicts the true effect from the data, and the histogram shows the distribution of the recovered effects from the model-generated data.

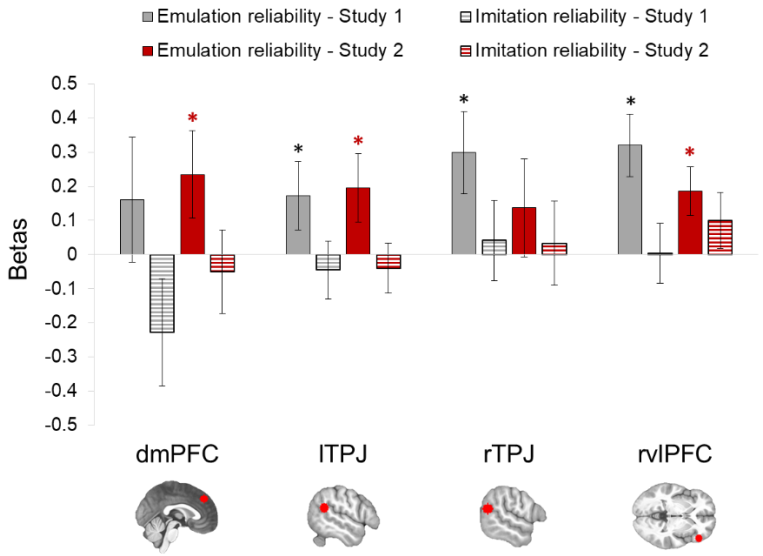

Figure S3, related to Figure 4. Reliability difference signals are only driven by positive tracking of emulation reliability. In Study 1, significant reliability difference signal was found in four ROIs: dmPFC, left and right TPJ, and right vlPFC. We extracted emulation (solid fill) and imitation (horizontal stripes fill) reliability signals separately in each of these ROIs and for each study (Study 1: grey, Study 2: red), to test whether the reliability difference signal is driven by both positive tracking of emulation reliability and negative tracking of imitation reliability. However, we find that this was not the case, instead only emulation reliability was found to be significant represented in the ROIs. Error bars represent SEM. T-tests: * $P<0.05$. The same results were found using non-parametric permutation tests.

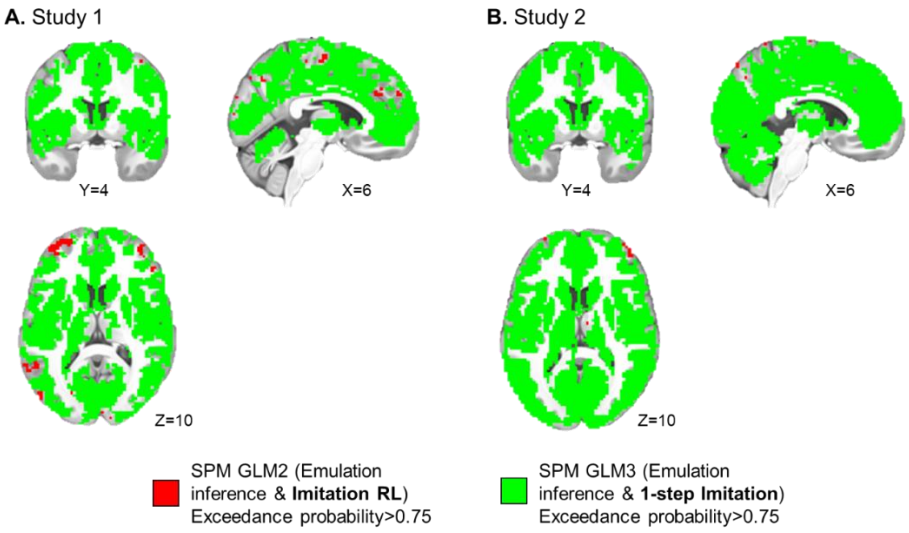

Figure S4, related to Figures 6 & 7. fMRI Bayesian Model Selection results. Grey matter voxels with exceedance probabilities greater than 0.75 are shown, in red for SPM GLM2 (representation of emulation inference signals and imitation RL signals) and in green for SPM GLM3 (representation of emulation inference signals and 1-step imitation signals). In both Study 1 (**A**) and Study 2 (**B**), SPM GLM3 was found to provide a better account of variations in the BOLD signal in a vast majority of grey matter voxels.

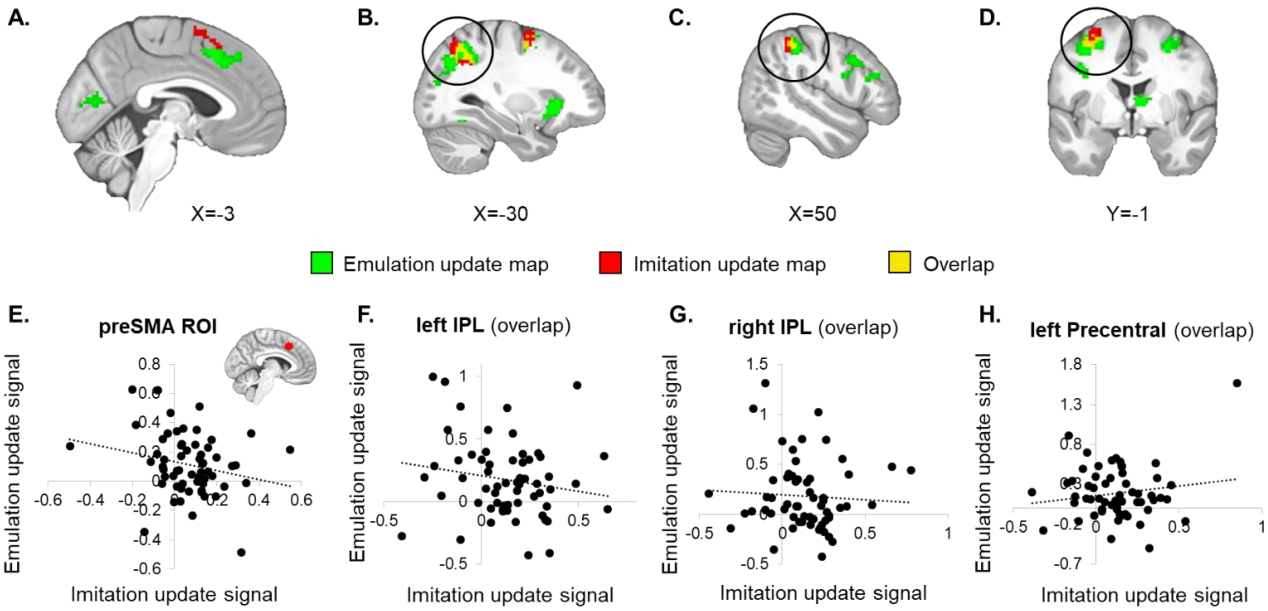

Figure S5, related to Figure 7. Overlap between emulation and imitation update signals. (**A-D**) The emulation update map (KL divergence over token values, shown on main text **Figure 7C**) and the imitation update map (action change relative to previous trial, shown on main text **Figure 7G**) from SPM GLM 3 were overlaid. Emulation signal is shown in green, imitation signal in red and the overlap in yellow. (**A**) Both update signals recruited the preSMA ROI, but in fact showed no overlap, with the emulation update signal more anterior and ventral than the imitation update signal. (**B-D**) Overlap was observed in three regions: (**B**) left inferior parietal lobule (60 voxels; peak: -30, -56, 43), (**C**) right inferior parietal lobule (44 voxels; peak: 48, -39, 46), and (**D**) left precentral/mid-frontal gyrus (33 voxels; peak: -33, -1, 53). (**E-H**) Extracting the two signals from (**E**) the preSMA ROI or (**F-H**) the overlapping voxels in the three regions described above showed no significant correlation across participants (**E**: R_{60} = -0.227, P=0.082; **F**: R_{60} = -0.175, P=0.18; **G**: R_{60} = -0.057, P=0.66; **H**: R_{60} = 0.150, P=0.25).

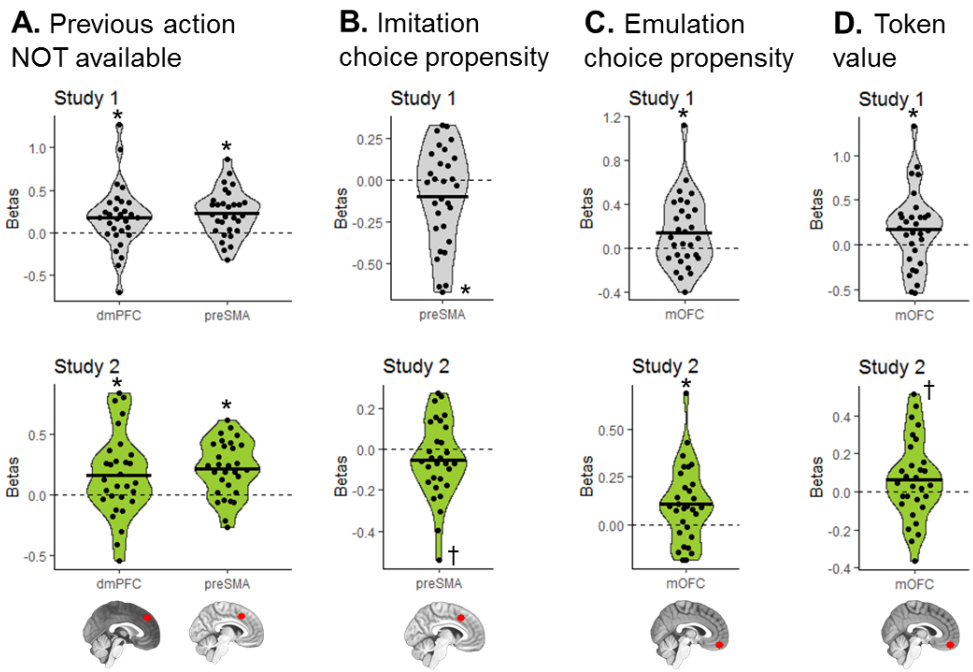

Figure S6, related to Figures 6 & 7. SPM GLM3 additional contrasts ROI results. Mean signal was extracted from pre-registered ROIs for each remaining contrast of interest in SPM GLM3 not shown on main text **Figures 6-7**: (**A**) whether the partner's previous action is unavailable (vs available) on the current trial, (**B-C**) the probability to choose according to imitation (**B**) or emulation (**C**) at the time of self-choice, and (**D**) the value of the token shown on screen during token presentation. Regions with significant signals in Study 1 (top panels), plotted in grey, were selected as hypotheses and a priori ROI for Study 2 (bottom panels). Dots represent individual subjects and the black bar represents the mean beta value for each regressor. T-tests: * $P<0.05$, † $P\leq0.07$. The same results were found using non-parametric permutation tests.

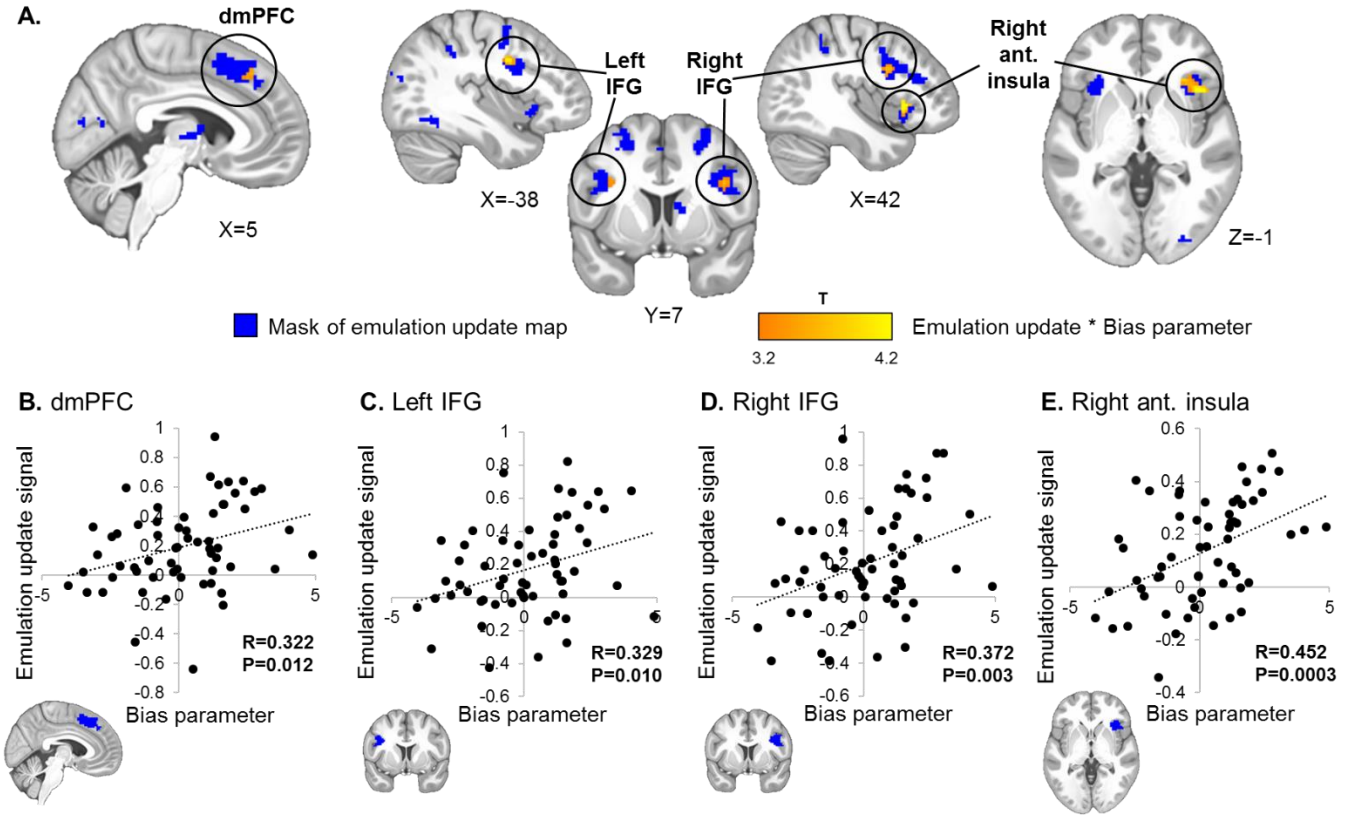

Figure S7, related to Figure 7. Individual bias towards emulation is reflected in the strength of the emulation update signal. (**A**) A second-level model was constructed to investigate whether individual differences in the bias parameter δ (extracted for each subject from the winning arbitration Model 10; high values reflect bias towards emulation) were associated with emulation update signals (token KL divergence at the time of feedback). In all 60 participants, the bias parameter δ was added as a covariate of the emulation update signal, controlling for study group. The resulting positive correlation map was then masked by the emulation update conjunction map (shown in **Fig. 7C** and in blue here), at P<0.001 uncorrected and k>10 contiguous voxels. Yellow clusters show voxels that not only significantly track emulation update but also in which the strength of this signal positively correlates with the behavioral bias towards emulation across individuals. (**B-E**) Emulation update betas were extracted for each subject from the four regions in which a positive correlation with the bias was found, namely dmPFC (**B**), left IFG (**C**), right IFG (**D**) and right anterior insula (**E**), and correlated with individual bias parameter values. Note that the map used to define the functional regions of interested was the emulation update conjunction map (blue clusters), not the correlation map, therefore the statistical inference associated with these correlations is not circular.

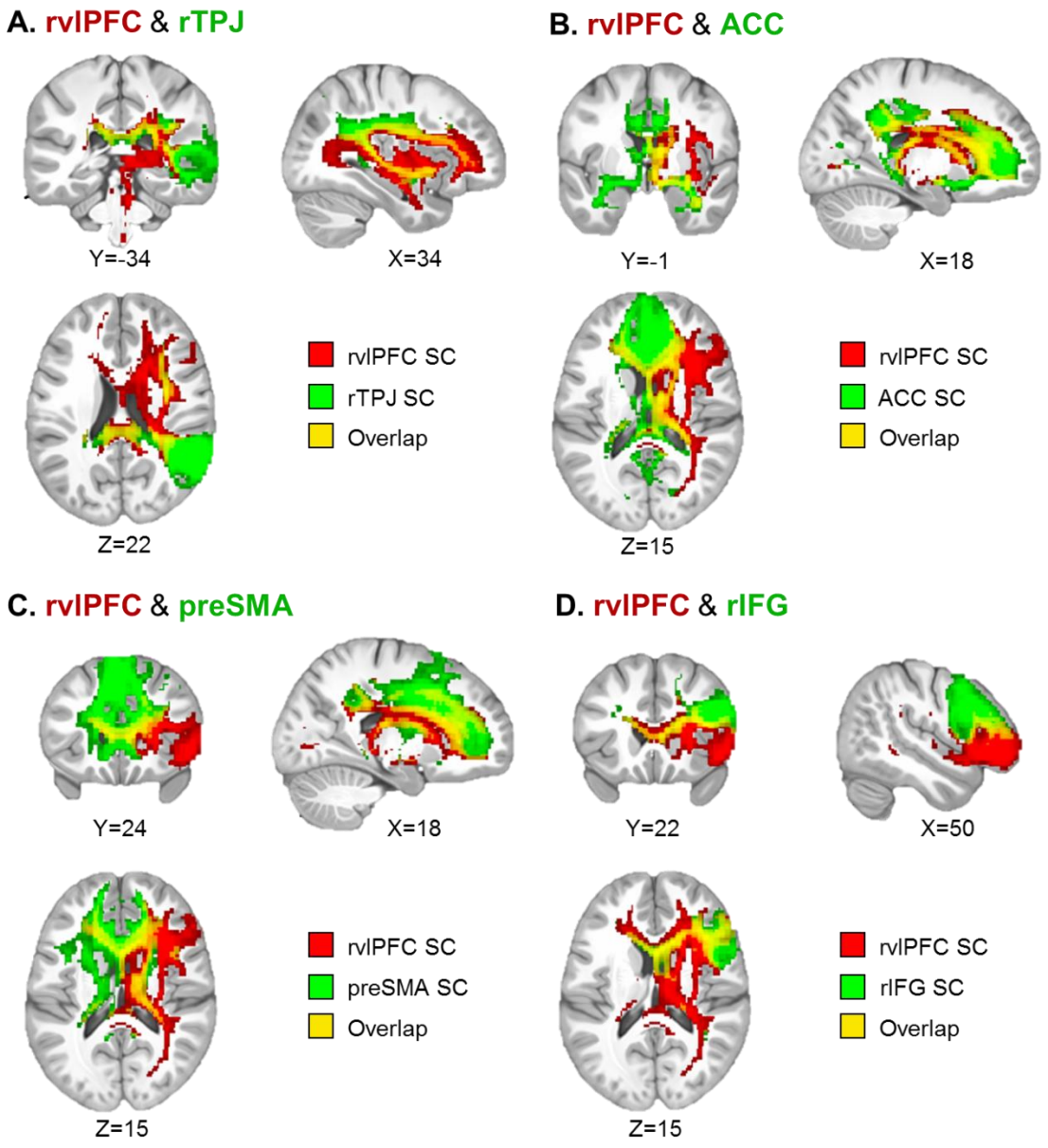

Figure S8, related to Figures 6 & 7. Structural connectivity patterns between regions of interest. The Brainnetome Atlas (http://atlas.brainnetome.org/index.html) was used to assess probabilistic structural connectivity patterns and ensure some of the regions we speculate may act as "hubs" to integrate imitation- and emulation-related signals are anatomically connected. For each region of interest, we selected the corresponding parcel (out of 246 sub-regions) from the atlas and overlaid the probabilistic structural connectivity maps (range: 0.5-1) between four example pairs of regions, all involving the right vlPFC (parcel #36): right TPJ (**A**, parcel #144), ACC (**B**, parcel #188), preSMA (**C**, parcel #1), and right IFG (**D**, parcel #30). Overlapping structural connectivity tracts are shown in yellow, suggesting that there is substantial anatomical connectivity in these pairs of regions and that they may all constitute relevant targets to explore for future functional and effective connectivity analyses.